

# Bidirectional AC-DC Converter for Regenerative Braking

Predrag Pejovic, Johann W. Kolar, and Yasuyuki Nishida

**Abstract**—In this paper, a bidirectional AC DC converter is analyzed. The converter applies a half bridge thyristor rectifier and a recuperating thyristor bridge instead of a braking resistor. Recuperating mode of the converter is focused in the analysis, and it is shown that the converter exposes two operating modes within the recuperating mode, one characterized by negligible, and the other one characterized by significant distortion of the input voltages. Theoretical results are experimentally verified on a 10 kW converter.

**Index Terms**—About four key words or phrases in alphabetical order, separated by commas.

## I. INTRODUCTION

IN this paper, a half-bridge three-phase thyristor rectifier intended for application in machine drives, presented in Fig. 1, is analyzed. In many applications, like crane [1] or elevator drives, a machine drive that presents the load operates in generating mode, and the generated energy requires to be taken care of. One method to do this is to dissipate the generated power on a pulse width modulated braking resistor ([2], page 421). This method is reliable, simple, and robust, but requires additional cooling effort, significantly reduces the converter power density, and increases the energy cost. To avoid these drawbacks, bidirectional power converters are of interest. Full-bridge thyristor rectifiers are simple and robust, and provide bidirectional power flow, but in the inverting mode the output voltage has to be reversed [3], [4]. Refinements of this approach can be found in [5], [6], and [7]. To keep the voltage polarity in the inverter mode, auxiliary thyristor bridge accompanied by a free-wheeling diode (Fig. 1) is proposed to replace the braking resistor voltage by the highest of the line voltages available at given time instant [8], [9]. Results presented in this paper are an extension of the results presented in [8] and [9], in theoretical direction, with

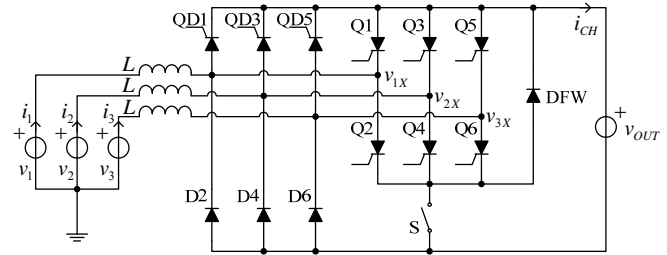


Fig. 1. The converter.

the converter control and operating modes subjected to detailed analysis.

## II. NOTATION AND NORMALIZATION

Let us assume that the converter is supplied by an undistorted symmetrical three-phase voltage system

$$v_k = V_m \cos\left(\omega t - (k-1)\frac{2\pi}{3}\right) \quad (1)$$

for  $k \in \{1, 2, 3\}$ . The supply lines are assumed to have leakage inductance  $L$  per phase, connected in series to the ideal voltage sources  $v_1$ ,  $v_2$ , and  $v_3$ . To simplify the notation, let us introduce two waveforms, one of them being the waveform of the voltage equal to the maximum of the phase voltages,

$$v_A = \max(v_1, v_2, v_3) \quad (2)$$

while the other one being the waveform of the voltage equal to the minimum of the phase voltages,

$$v_B = \min(v_1, v_2, v_3) \quad (3)$$

Since the phase voltages add up to zero,

$$v_1 + v_2 + v_3 = 0 \quad (4)$$

waveform of the voltage defined to be equal to the phase voltage that is neither minimal nor maximal at a considered time point can be obtained as

$$v_C = -v_A - v_B \quad (5)$$

According to the definitions of  $v_A$ ,  $v_B$ , and  $v_C$ , phase angle segments over the line period could be identified where indices of the phase voltages that represent  $v_A$ ,  $v_B$ , and  $v_C$  do not change. There are six such segments, and they are given in Table 1. Table 1 also contains values of the index variables  $A$ ,  $B$ , and  $C$ . For example, consider maximum of the line voltages  $v_{AB} = v_A - v_B$  on the segment  $\pi/3 < \omega t < 2\pi/3$ ; in that segment,  $v_{AB} = v_2 - v_3$ , since  $A=2$  and  $B=3$  over the segment. Besides the values of the phase voltage index variables, Table I also contains values of semiconductor index

Manuscript received 30 May 2012. Accepted for publication 10 June 2012. Some results of this paper were presented at the 16th International Symposium Power Electronics, Novi Sad, Serbia, October 26-28, 2012.

P. Pejović is with the Faculty of Electrical Engineering, University of Belgrade, Belgrade, Serbia (phone: +381-11-3218-313; fax: +381-11-324-8681; e-mail: peja@etf.rs).

J. W. Kolar is with Swiss Federal Institute of Technology, Zürich, Switzerland (e-mail: kolar@lem.ee.ethz.ch).

Y. Nishida is with the Chiba Institute of Technology, Japan (e-mail: nishida\_yas@nifty.com).

TABLE I  
DEFINITIONS OF INDEX VARIABLES,  $A, B, C, a$ , AND  $b$

| range                        | $A$ | $B$ | $C$ | $a$ | $b$ |
|------------------------------|-----|-----|-----|-----|-----|
| $0 < \omega t < \pi/3$       | 1   | 3   | 2   | 1   | 6   |
| $\pi/3 < \omega t < 2\pi/3$  | 2   | 3   | 1   | 3   | 6   |
| $2\pi/3 < \omega t < \pi$    | 2   | 1   | 3   | 3   | 2   |
| $\pi < \omega t < 4\pi/3$    | 3   | 1   | 2   | 5   | 2   |
| $4\pi/3 < \omega t < 5\pi/3$ | 3   | 2   | 1   | 5   | 4   |
| $5\pi/3 < \omega t < 2\pi$   | 1   | 2   | 3   | 1   | 4   |

variables  $a$  and  $b$ , where  $a$  is the index of the semiconductor component connected to the highest of the phase voltages, while  $b$  is the index of the of the semiconductor component connected to the lowest of the phase voltages.

Since numerical methods were extensively used to provide the results presented in this paper, to generalize the results normalization of variables is introduced. The voltages are normalized taking amplitude of the phase voltage as a basis, providing normalized value  $m_X$  of the voltage  $v_X$  as

$$m_X = \frac{v_X}{V_m} \quad (6)$$

The currents are normalized taking amplitude of the short-circuit phase current as a base current for normalization

$$j_X = \frac{\omega L}{V_m} i_X \quad (7)$$

The base current for normalization is high, thus all the currents in the analysis would be characterized by relatively low per unit values. For example, the RMS value of the phase short-circuit current is

$$I_{SC\,RMS} = \frac{1}{\sqrt{2}} \frac{V_m}{\omega L} \approx 0.707 \text{ p.u.} \quad (8)$$

A consequence is that the powers in the system would also be characterized by low per unit quantities, thus the short circuit apparent power is

$$S_{SC} = \frac{3}{2} \frac{V_m^2}{\omega L} = 1.5 \text{ p.u.} \quad (9)$$

Applying normalization defined by (6) and (7), the equation that characterizes the line inductance

$$v_L = L \frac{di_L}{dt} \quad (10)$$

in normalized terms becomes

$$m_L = \frac{dj_L}{d\omega t} \quad (11)$$

In analyses that follow, time variable  $t$  will be frequently represented by the phase angle variable  $\omega t$ , like it has already been done in (11).

### III. ANALYSIS OF THE CONVERTER OPERATION

Fundamental idea discussed in this paper is how to replace the voltage across the braking resistor with the maximum of the line voltages,  $v_{AB}$ , obtained applying the recuperating thyristor bridge of Fig. 1? Besides the voltage  $v_{AB}$ , the

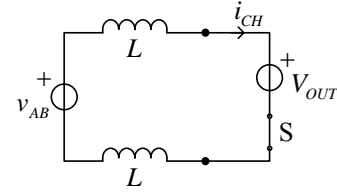


Fig. 2. Equivalent circuit of the converter during the recuperation interval.

recuperating thyristor bridge provides connection to two  $L$  inductors that represent the line inductance, connected in series to  $v_{AB}$ , as depicted in Fig. 2. In the analysis, it is assumed that the output voltage is constant. Thus, the output of the converter, including the output capacitor, is replaced by a constant voltage source  $V_{OUT}$  in the circuit diagram of Fig. 1, being supplied by the charging current  $i_{CH}$ , as depicted in Fig. 2.

According to the phase voltages (1), on the phase angle segment  $0 < \omega t < \pi/3$  maximum of the line voltages is given by its normalized value

$$m_{AB}(\omega t) = \sqrt{3} \sin\left(\omega t + \frac{\pi}{3}\right) \quad (12)$$

reaching the minimum of  $m_{AB}(0) = m_{AB}(\pi/3) = 1.5$ . Now, let us assume that in the phase angle interval  $0 < \omega t < \alpha$  the braking switch of Fig. 1 is on, and that  $M_{OUT} > m_{AB}$ , which results in the recuperation interval. During the interval, normalized equation that characterizes the charging current is

$$\frac{dj_{CH}}{d\omega t} = \frac{1}{2}(m_{AB} - M_{OUT}) \quad (13)$$

Assuming that  $j_{CH}(0) = 0$ , the waveform of  $j_{CH}$  is given by

$$j_{CH}(\omega t) = -\frac{1}{2} \left[ \sqrt{3} \cos\left(\omega t + \frac{\pi}{3}\right) + M_{OUT} \omega t - \frac{\sqrt{3}}{2} \right] \quad (14)$$

which for  $M_{OUT} > \sqrt{3}$  reaches maximum of its magnitude for  $\omega t = \alpha$ ,  $j_{MAX} = -j_{CH}(\alpha)$ .

Average of the charging current is computed performing averaging over the phase angle of  $\pi/3$ , which is the phase angle interval that corresponds to the fundamental period of the charging current,

$$J_{CH} = \frac{3}{\pi} \int_0^{\alpha} j_{CH}(\omega t) d\omega t \quad (15)$$

resulting in

$$J_{CH} = \frac{3}{4\pi} \left( 2\sqrt{3} \sin\left(\alpha + \frac{\pi}{3}\right) + M_{OUT} \alpha^2 - \sqrt{3} \alpha - 3 \right) \quad (16)$$

In steady state, the converter output current is equal to the average of the charging current,  $J_{OUT} = J_{CH}$ , according to the charge balance over the filtering capacitor connected in parallel to the load. This is not shown in Fig. 1, but being assumed.

The charging current (16) is negative, which corresponds to the converter operation in the inverting mode. Normalized

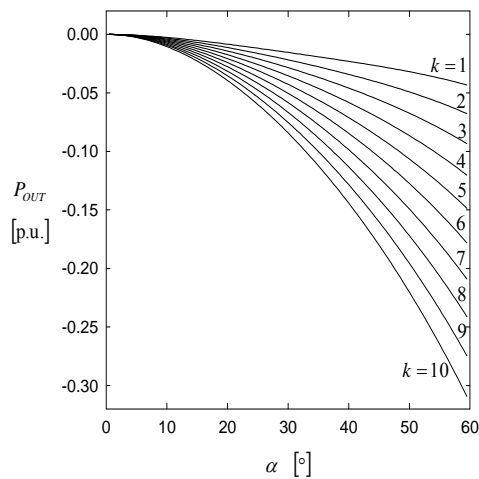


Fig. 3. Dependence of  $P_{OUT}$  on  $\alpha$  for  $M_{OUT} = 1.7 + 0.05k$ .

power in the inverting mode is given by  $P_{OUT} = M_{OUT} J_{CH}$ , and for various values of  $M_{OUT}$  and  $\alpha$  it is depicted in Fig. 3. From the curves of Fig. 3 it can be observed that relatively high power could be recuperated, and that the process could be controlled varying the switch on-angle  $\alpha$ , being also dependent on the converter output voltage.

Averaged equation over the output capacitor voltage governs the converter output voltage, and in normalized form it is given by

$$\frac{d m_{OUT}}{d \omega t} = j_{CH}(m_{OUT}, \alpha) - j_{OUT} \quad (17)$$

Thus, dynamics of the converter in the recuperation mode is given by the first order nonlinear differential equation.

The analysis performed this far covers only the recuperating interval. However, at the end of the interval substantial amount of energy might remain stored in the inductors of

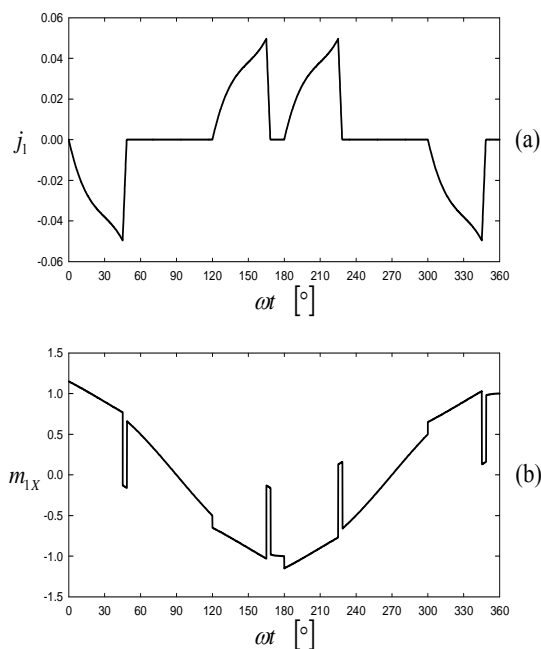
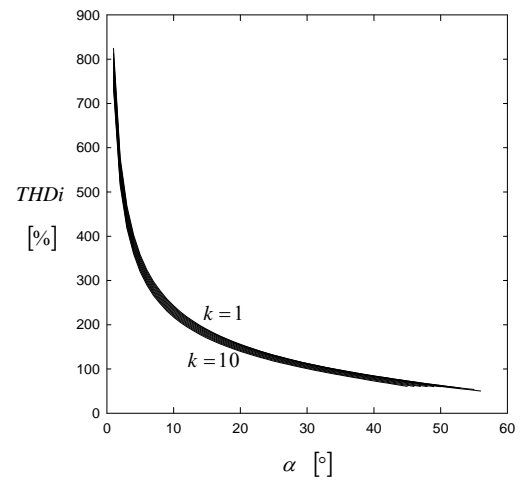
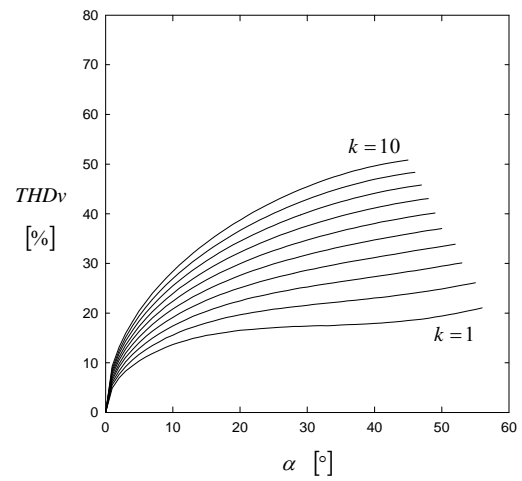


Fig. 4. Waveforms of  $j_1$  and  $m_{1X}$  for  $M_{OUT} = 1.8$  and  $\alpha = 45^\circ$ .



(a)



(b)

Fig. 5. Dependence of the input current (a) and the coupling point voltage (b) THD on  $\alpha$  for  $M_{OUT} = 1.7 + 0.05k$ .

Fig. 2. For example, for  $M_{OUT} > \sqrt{3}$  the maximum of  $|i_{CH}|$  flows through the inductors at the time instant when S is being turned off. This energy will be discharged through the free-wheeling diode (DFW in Fig. 1) during the discharge interval that follows the recuperating interval. Equivalent circuit for this interval corresponds to the circuit diagram of Fig. 2 with  $V_{OUT}$  replaced by a short circuit, and the governing equation for the current of the inductors  $i_L$  is

$$\frac{d j_L}{d \omega t} = \frac{1}{2} m_{AB} \quad (18)$$

where  $i_L$  is oriented in the same direction as  $i_{CH}$ . This interval lasts while  $i_L < 0$ . The discharge interval does not contribute to the recuperated power, since the voltage source that represents the load, is open during the interval. Typical waveforms of  $j_1$  and  $m_{1X}$  in the recuperating mode are shown in Fig. 4.

Dependence of the input current THD and the THD of the voltages at the converter coupling points, just after the inductors that represent leakage inductances of the line, are

presented in Fig. 5. The converter is characterized by high distortions of the currents and voltages, which might not be a fact of relevance in isolated local networks.

#### IV. CONTROL OF THE CONVERTER

In the analysis presented this far, it was shown that the output voltage could be controlled adjusting the switch on angle  $\alpha$ , and that the governing equation is a nonlinear first order differential equation (17). In this section, the analysis is extended to the output voltage below  $M_{OUT} = \sqrt{3}$ , down to  $M_{OUT} = 1.5$ , which is the bottom limit to turn the thyristors Q1 to Q6 on. In this case, the charging current  $i_{CH}$  may reach zero spontaneously, causing the thyristors of the recuperating

bridge to turn off, without any need for hard switched turn off of S. This operating mode is named soft discharge mode.

According to (13), at low output voltages, lower than  $\sqrt{3}$  p.u., recuperating current grows in magnitude as long as  $m_{AB} < M_{OUT}$ , while it starts to decrease when  $m_{AB} > M_{OUT}$ . For the output voltages lower than about 1.67 p.u., the recuperating current reaches to zero during the recuperating interval, and the thyristors Qa and Qb turn off spontaneously. Exact limit of this operating mode is  $M_{OUT} < M_{SDM}$ , where  $M_{SDM}$  is obtained as a solution of

$$M_{SDM} \arcsin \frac{M_{SDM}}{\sqrt{3}} + \sqrt{3 - M_{SDM}^2} - \frac{2\pi}{3} M_{SDM} + \frac{\sqrt{3}}{2} = 0 \quad (19)$$

Numerical solution of (19) is  $M_{SDM} \approx 1.673436$ . In the case  $M_{OUT} < M_{SDM}$ , the line inductance discharge is spontaneously performed. In this manner, the voltage spikes related to the discharge process after the hard turn off of S are avoided, and the THD of the input voltages remains moderate. In the first two diagrams of Fig. 6, the input current and the input voltage are presented for the converter operating in this mode, at  $M_{OUT} = 1.65$  and  $\alpha = 45^\circ$ , corresponding to  $J_{OUT} = -0.023$ . The THD of the input current, presented in Fig. 6(a), was expectedly high, equal to 127%. However, the THD of the input voltage waveform, presented in Fig. 6(b), was only 2.73%, which is a consequence of the absence of the voltage spikes that characterize the discharge process caused by hard

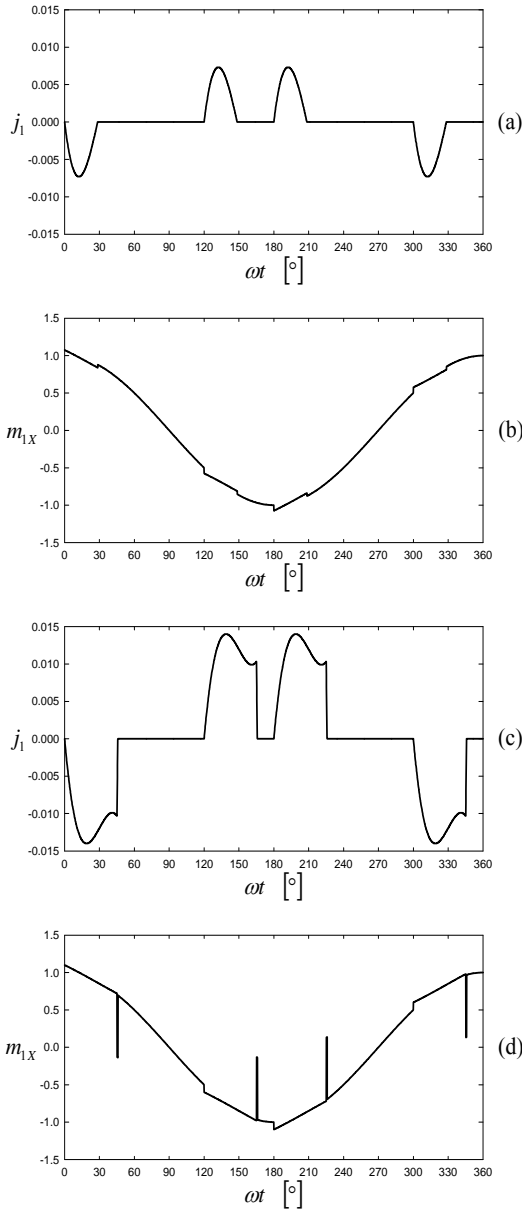


Fig. 6. Waveforms of the input current and the input voltage for  $\alpha = 45^\circ$ : (a) and (b) soft discharge mode at  $M_{OUT} = 1.65$ ; (c) and (d) hard discharge mode at  $M_{OUT} = 1.7$ .

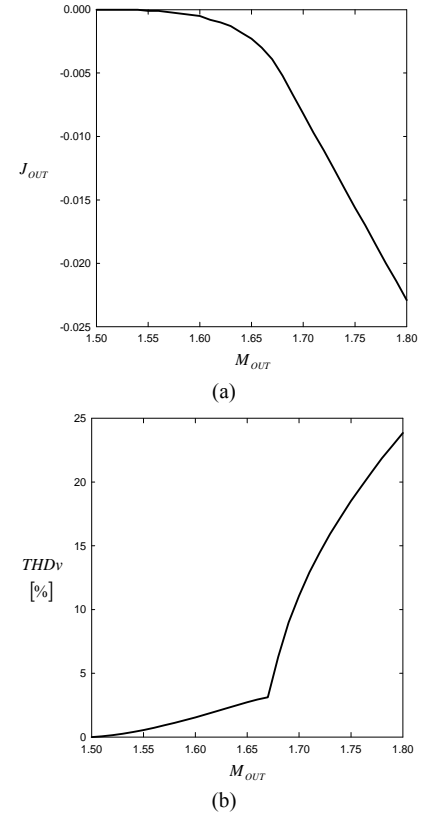


Fig. 7. (a) Dependence of  $J_{OUT}$  on  $M_{OUT}$  for  $\alpha = 45^\circ$ ; (b) dependence of the input voltage THD on  $M_{OUT}$  for  $\alpha = 45^\circ$ .

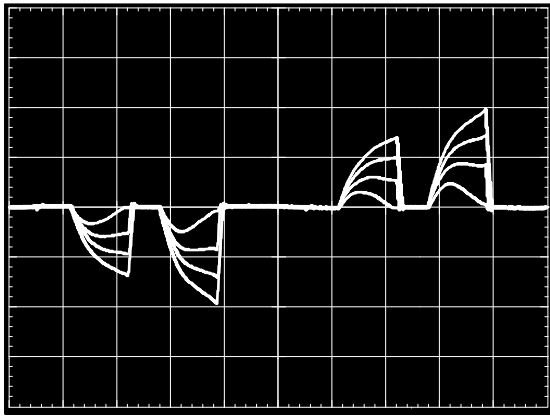


Fig. 8. Waveforms of the input current for the output voltages of 590 V, 580 V, 570 V, and 550 V. Scales: 20 A/div, 2 ms/div.

turn off of S. Applying numerically obtained value for  $M_{SDM}$ , maximum of the recuperated current absolute value in the soft discharge mode is obtained as  $J_{OUT} = -0.004291$ , which corresponds to the recuperated power of  $P_{OUT} = -0.007181$  p.u., or in the terms of the short circuit apparent power at the point of coupling

$$\frac{P_{OUT}}{S_{SC}} = -0.4787\% \quad (20)$$

Output current of recuperating mode increased above the soft discharge limit forces the converter to operate in the hard discharge mode. The input current and the input voltage waveforms that correspond to this operating mode at  $M_{OUT} = 1.7$  and  $\alpha = 45^\circ$ , corresponding to  $J_{OUT} = -0.0081$ , are presented in the last two diagrams of Fig. 6, labeled (c) and (d). The THD of the input current is reduced to 69.44%, while the THD of the input voltage is increased to 11.77%.

In order to compare the converter behavior in the soft discharge mode to the operation in the hard discharge mode, a set of numerical simulations is performed. In Fig. 7(a) dependence of the recuperated current  $J_{OUT}$  on the output voltage  $M_{OUT}$  is presented. It can be observed that for normalized output voltages lower than  $M_{SDM}$  absolute value of the recuperated output current is relatively low in magnitude, lower than the limit of 0.00429 p.u. Increased output voltage causes the converter to operate in the hard discharge mode, resulting in increased absolute value of the recuperated current. In Fig. 7(b), dependence of the input voltage THD on the output voltage is presented. Point where the converter switches from soft discharge mode to the hard discharge mode is readily observable by sudden increase of the input voltage THD.

It can be concluded that the converter at low output voltages and relatively low recuperating power could be operated in the soft discharge mode, which is characterized by absence of the input voltage spikes and moderate distortions of the input voltages. Besides, hard switched turn off of S is avoided in this mode. In the case the load tolerates the output voltage variations of about 20%, it is possible to operate the

converter with a constant on-angle of S. In that case, at higher recuperating power the converter would operate in the hard discharge mode, while at lower recuperating power the converter would operate in the soft discharge mode.

## V. EXPERIMENTAL RESULTS

In order to verify feasibility of the proposed concept, a laboratory model of the converter with the rated power of 10 kW was built applying IXYS VVZB 120 module for the half controlled thyristor bridge and the controlled switch, and six discrete thyristors IXYS CS 30-120i, for the recuperating thyristor bridge. The converter is intended to operate at the three-phase voltage system with the phase voltage RMS value of 230 V, at 50 Hz. The line inductance was 1 mH. The output voltage of the converter was impressed by an external DC source, which is applied to provide the power to be recuperated to the mains. To analyze the effects caused by the supplying three-phase voltage system unbalance, voltage at one of the phases is increased for about 4% by an adjustable transformer.

To illustrate the converter operation at different output voltages, while keeping the switch on-angle constant, a set of measurements is performed, and obtained waveforms of the input currents are presented in Fig. 8. The measurements are performed for four values of the output voltage: 590 V, 580 V, 570 V, and 550 V. These output voltages correspond to the recuperating power of 9.3 kW, 7.2 kW, 5.4 kW, and 1.6 kW, respectively. Operation of the converter in the soft discharge mode at the lowest of the power is clearly observable.

## VI. CONCLUSIONS

In this paper, a bidirectional AC-DC converter intended for application in machine drives to provide regenerative braking is analyzed. The converter is derived replacing the braking resistor by a thyristor bridge that provides the maximum of the line voltages at its output in order to recuperate the braking energy. Appropriate normalization is introduced to generalize the results. Operation of the converter is analyzed in detail, and it is shown that the converter in the recuperating mode can operate in two sub-modes: soft discharge mode and the hard discharge mode. The soft discharge mode is shown to provide recuperation with negligible distortion of the input voltages. Limits for this operating mode are derived. Constant on angle control strategy for the recuperating switch is analyzed, and it is shown to be applicable for the loads that tolerate 20% variation of the supply voltage. The analyses are experimentally verified on a 10 kW converter laboratory model.

## REFERENCES

- [1] R. Belmans, F. Busschots, R. Timmer, "Practical design considerations for braking problems in overhead crane drives," in IEEE Industry Applications Society Annual Meeting, 1993, pp. 473-479.

- [2] N. Mohan, T. M. Undeland, W. P. Robbins, *Power Electronics: Converters, Applications and Design*, 2nd Edition. New York: John Wiley & Sons, 1995.
- [3] R. M. Davis, "A bidirectional AC DC power converter for fixed polarity DC loads," in 3rd International Conference on Power Electronics and Variable Speed Drives, London, UK, 1988, pp. 142-145.
- [4] D. Milly, "An AC to DC converter with output reversal," in Record of the 3rd European Conference on Power Electronics and Applications, Aachen, Germany, 1989, pp. 813-817.
- [5] J. C. Clare, P. R. Mayes, W.F. Ray, "Bidirectional power converter for voltage fed inverter machine drives," in 23rd Annual IEEE Power Electronics Specialists Conference Record, 1992, pp. 189-194.
- [6] K. Matsui, K. Tsuboi, S. Muto, "Power regenerative controls by utilizing thyristor rectifier of voltage source inverter," *IEEE Transactions on Industry Applications*, vol. 28, pp. 816-823, July/Aug. 1992.
- [7] K. Matsui, U. Mizuno, Y. Murai, "Improved power regenerative controls by using thyristor rectifier bridge of voltage source inverter and a switching transistor," *IEEE Transactions on Industry Applications*, vol. 28, pp. 1010-1016, Sep./Oct. 1992.
- [8] J. W. Kolar, H. Ertl, F. C. Zach, "A novel concept for regenerative braking of PWM-VSI drives employing a loss-free braking resistor," in 12th Annual Applied Power Electronics Conference and Exposition APEC '97 Conference Proceedings, 1997, pp. 297-305.
- [9] J. W. Kolar, H. Ertl, F. C. Zach, "Design and experimental evaluation of the loss-free braking resistor concept for applications in integrated converter machine systems," in Proceedings of the 24th Annual Conference of the IEEE Industrial Electronics Society, IECON '98, 1998, pp. 626-629.